RUDN university

UNIVERSITÉ DE LYON

International online workshop

Mathematical Modelling in Biomedicine

October 25 – 29, 2021 Moscow, Russia

The First Multi-Cellular Model of Neuroblastoma

K. Y. Wertheim, R. Chisholm, P. Richmond, D. Walker

University of Sheffield, Sheffield, South Yorkshire S10 2TN

k.wertheim@sheffield.ac.uk

The University Of Sheffield.

INSIGNEO

Institute for *in silico* Medicine

PRIMAGE

Medical imaging
Artificial intelligence
Childhood cancer research

Horizon 2020
European Union Funding
for Research & Innovation

Objectives

1. PRIMAGE project.

2. Scale separation strategy in the project.

3. The first multi-cellular model of neuroblastoma.

4. Model calibration using GPUs.

Objectives

1. PRIMAGE project.

2. Scale separation strategy in the project.

3. The first multi-cellular model of neuroblastoma.

4. Model calibration using GPUs.

Explainer

https://vimeo.com/613708072/c59c67572c or https://kywertheim.com/research/PrimageVideo.mp4

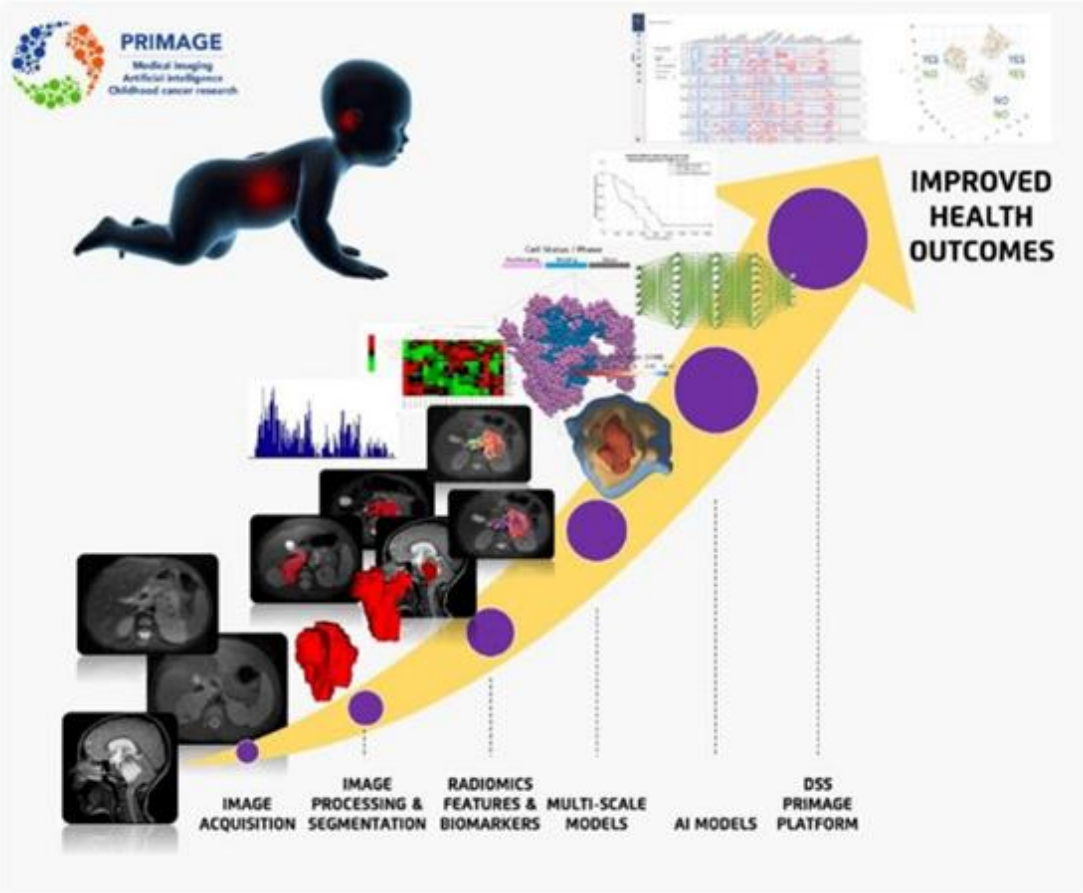

Martí-Bonmatí, Luis, et al. "PRIMAGE project: predictive in silico multiscale analytics to support childhood cancer personalised evaluation empowered by imaging biomarkers." *European radiology experimental* 4.1 (2020): 1-11.

Decision support system for the clinical management of malignant solid tumours.

1. Image acquisition, processing, and segmentation.

2. Integrate radiomic features with other biomarkers, such as mutations and histology.

3. **Multiscale models: organ/tumour, tissue, and intracellular.**

4. Machine learning techniques extract insights from simulation results.

Objectives

1. PRIMAGE project.

2. Scale separation strategy in the project.

3. The first multi-cellular model of neuroblastoma.

4. Model calibration using GPUs.

Neuroblastoma

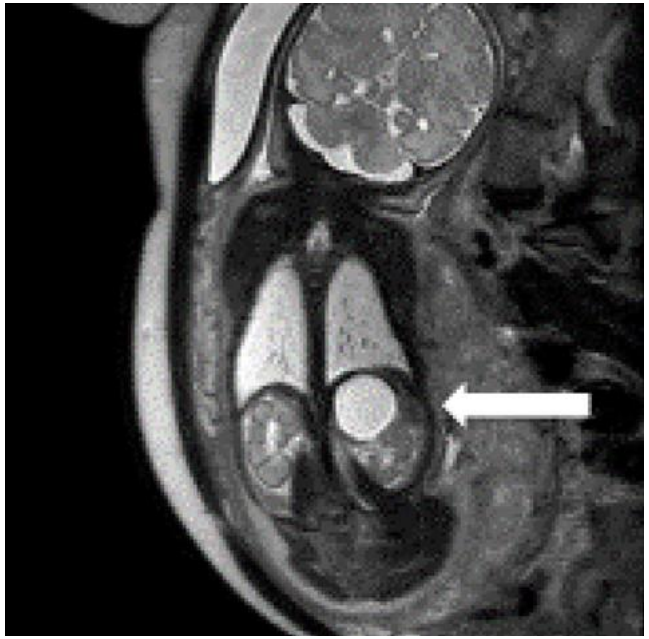

Louis, Chrystal U., and Jason M. Shohet. "Neuroblastoma: molecular pathogenesis and therapy." *Annual review of medicine* 66 (2015): 49-63.

Paediatric cancer:

- Most common extra-cranial solid tumour in children.
- 15 % of cancer-related deaths in children.
- Adrenal medulla is usually the primary site.

Neuroblastoma

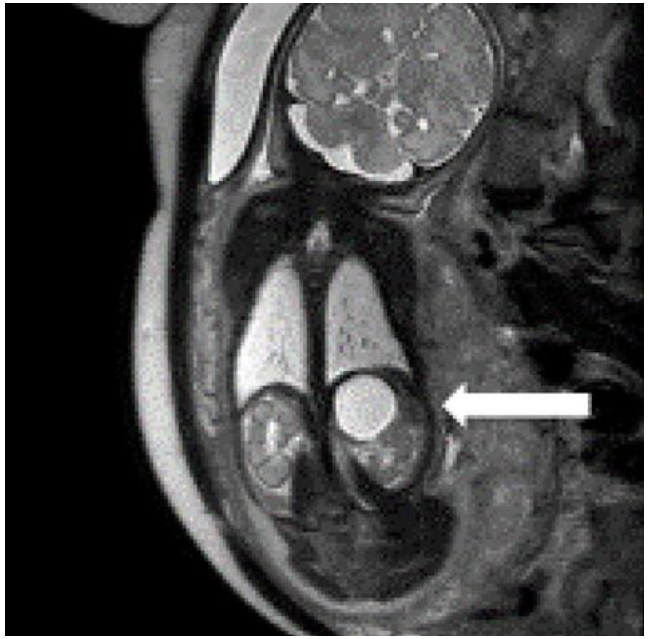

Louis, Chrystal U., and Jason M. Shohet. "Neuroblastoma: molecular pathogenesis and therapy." *Annual review of medicine* 66 (2015): 49-63.

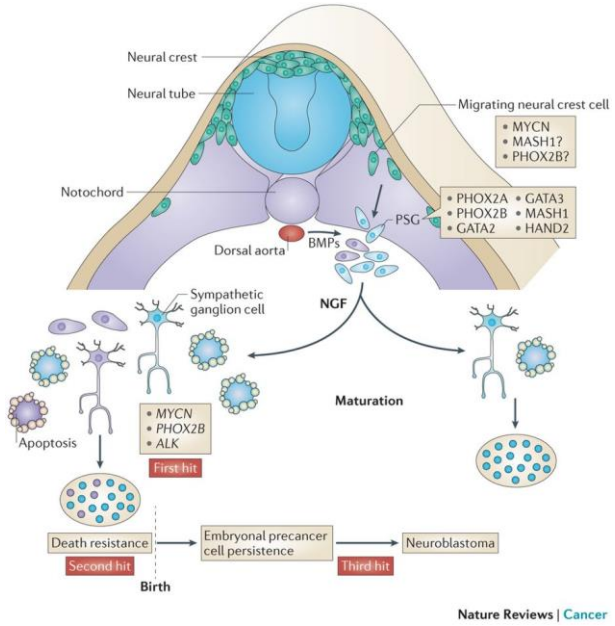

Marshall, Glenn M., et al. "The prenatal origins of cancer." *Nature Reviews Cancer* 14.4 (2014): 277-289.

Paediatric cancer:

- Most common extra-cranial solid tumour in children.
- 15 % of cancer-related deaths in children.
- Adrenal medulla is usually the primary site.

Neural crest:

- Transient structure during embryonic development.
- Migrate and differentiate into different cell types.
- Sympathetic nervous system.

Neuroblastoma

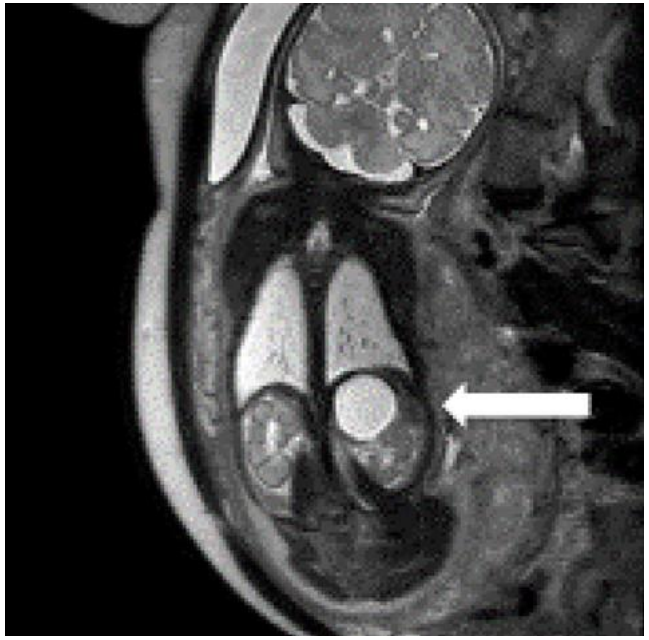

Louis, Chrystal U., and Jason M. Shohet. "Neuroblastoma: molecular pathogenesis and therapy." *Annual review of medicine* 66 (2015): 49-63.

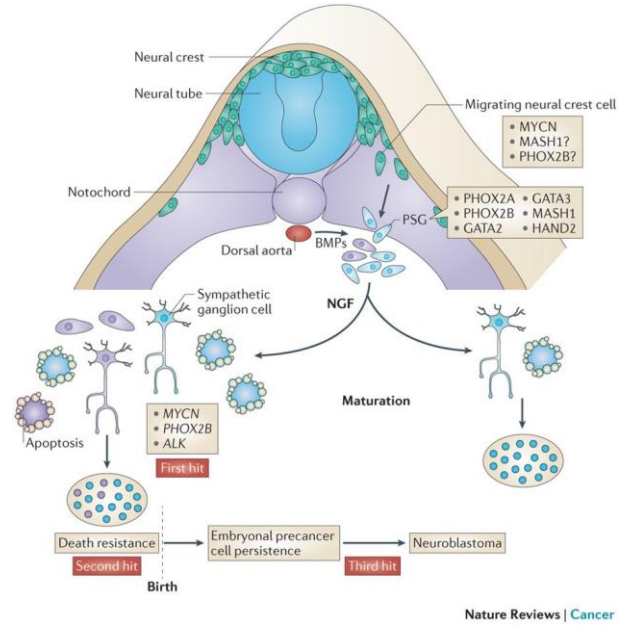

Marshall, Glenn M., et al. "The prenatal origins of cancer." *Nature Reviews Cancer* 14.4 (2014): 277-289.

INRG Stage	Age (months)	Histologic Category	Grade of Tumor Differentiation	*MYCN*	11q Aberration	Ploidy	Pretreatment Risk Group
L1/L2		GN maturing; GNB intermixed					A Very low
L1		Any, except GN maturing or GNB intermixed		NA			B Very low
				Amp			K High
L2	< 18	Any, except GN maturing or GNB intermixed		NA	No		D Low
					Yes		G Intermediate
	≥ 18	GNB nodular; neuroblastoma	Differentiating	NA	No		E Low
					Yes		H Intermediate
			Poorly differentiated or undifferentiated	NA			
				Amp			N High
M	< 18			NA		Hyperdiploid	F Low
	< 12			NA		Diploid	I Intermediate
	12 to < 18			NA		Diploid	J Intermediate
	< 18			Amp			O High
	≥ 18						P High
MS	< 18			NA	No		C Very low
					Yes		Q High
				Amp			R High

Sokol, Elizabeth, and Ami V. Desai. "The Evolution of Risk Classification for Neuroblastoma." *Children* 6.2 (2019): 27.

Paediatric cancer:

- Most common extra-cranial solid tumour in children.
- 15 % of cancer-related deaths in children.
- Adrenal medulla is usually the primary site.

Neural crest:

- Transient structure during embryonic development.
- Migrate and differentiate into different cell types.
- Sympathetic nervous system.

Heterogeneity:

- Spontaneous regression.
- Drug resistance and metastasis even after multi-modal treatment.
- MYCN amplification.
- < 50 % survival rate in high-risk cases.

Cancer hallmarks

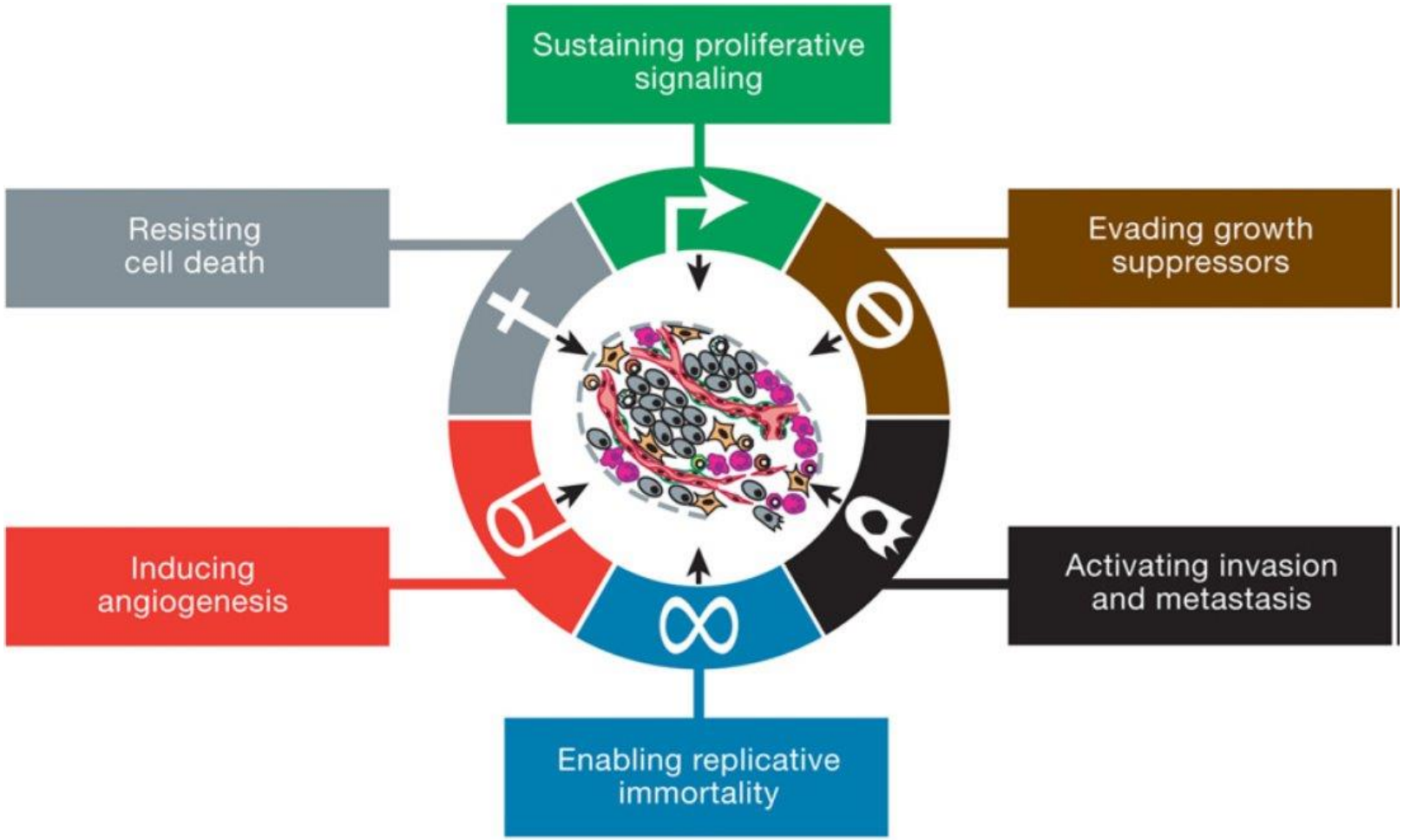

Hanahan, Douglas, and Robert A. Weinberg. "Hallmarks of cancer: the next generation." *cell* 144.5 (2011): 646-674.

Multiscale problem

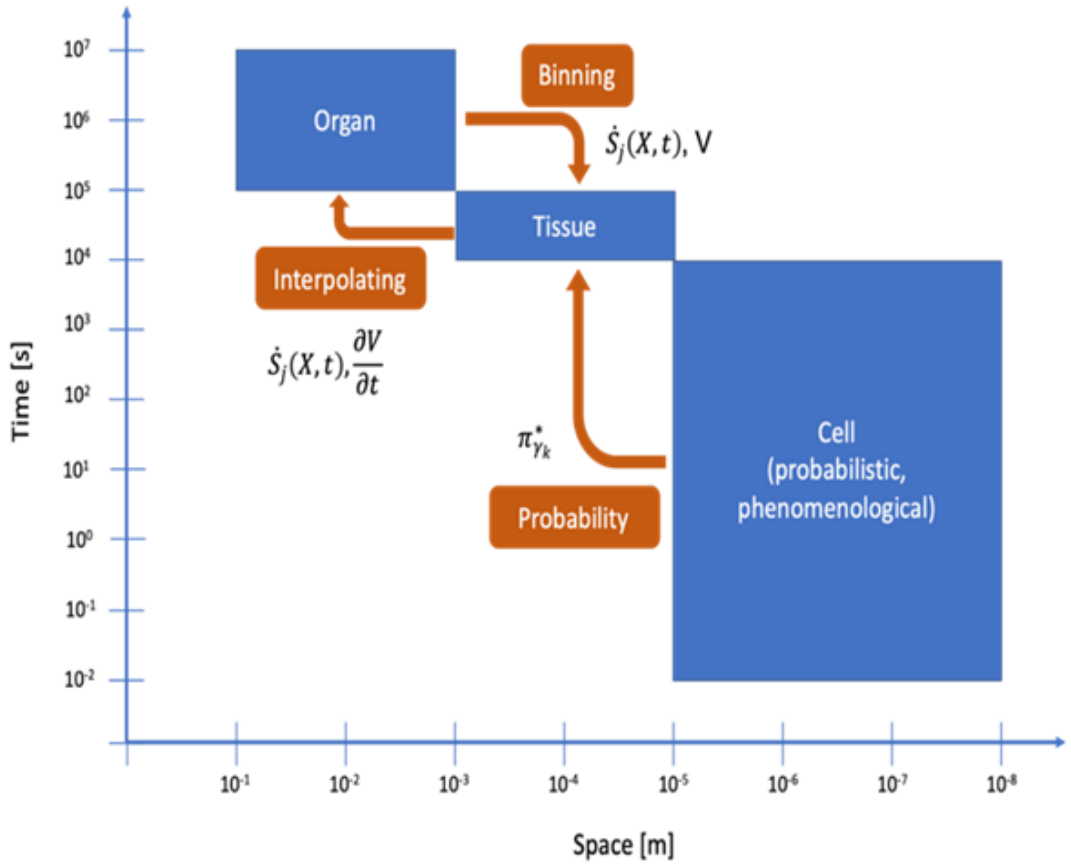

de Melo Quintela, B., Hervás-Raluy, S., Garcia-Aznar, J.M., Walker, D., Wertheim, K.Y., and Viceconti, M., 2021. A Theoretical Analysis of the Scale Separation in a Model to Predict Solid Tumour Growth. *Journal of Theoretical Biology*. Manuscript under review and available upon request.

Cannot describe biological phenomena spanning **nine orders of magnitude** in a single-scale model.

1. Experimental resolutions.
2. Model complexity.
3. Computational costs.

ALMA MATER STUDIORUM
UNIVERSITÀ DI BOLOGNA

Multiscale model

Tumour Tissue Cell

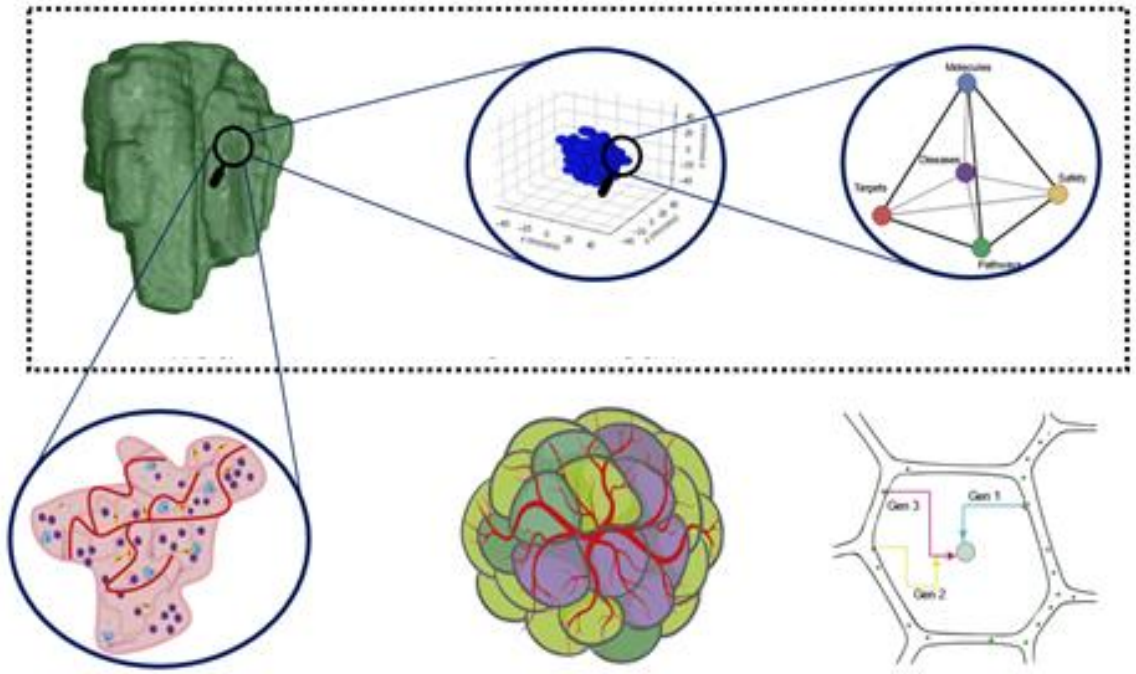

Partial differential equations.

Finite element method.

Discrete agents, continuous automaton, and centre-based mechanical model.

Monte Carlo method.

Statistical and machine learning models.

Universidad Zaragoza 1542

Chemotargets

Objectives

1. PRIMAGE project.

2. Scale separation strategy in the project.

3. The first multi-cellular model of neuroblastoma.

4. Model calibration using GPUs.

Model structure

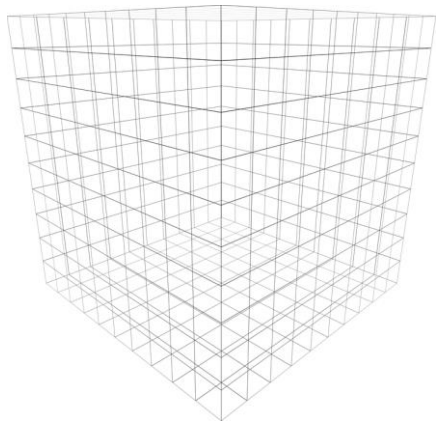

Part 1: continuous automaton.

- Voxelate the tumour microenvironment.
- Spatial distributions of cells and matrix.
- Oxygen, nutrients, and chemotherapeutic drugs (uniform).
- Inflammation (uniform).

Model structure

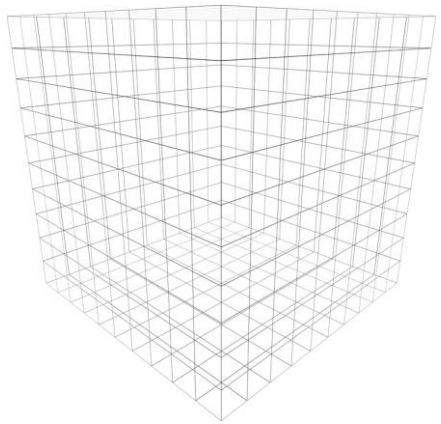

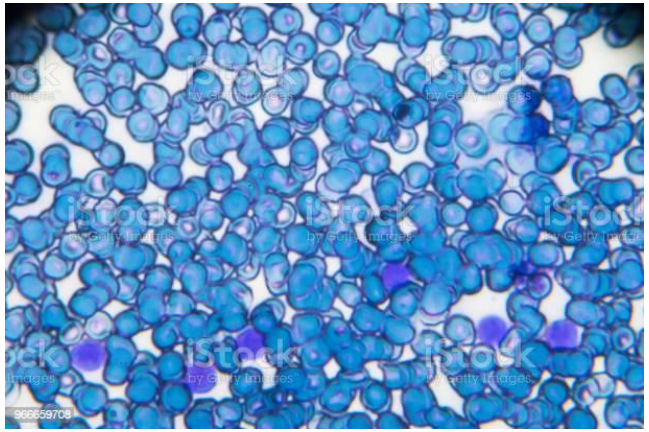

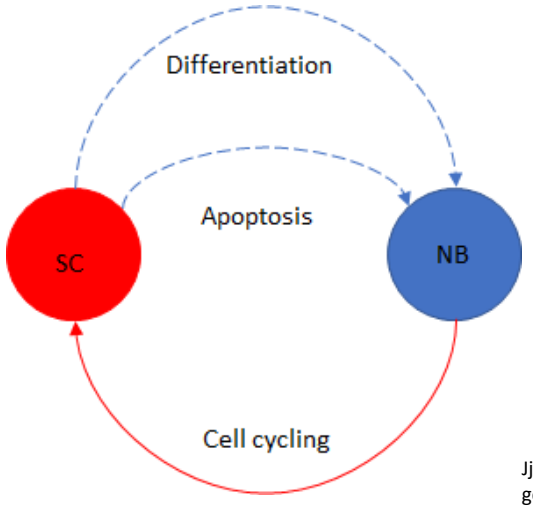

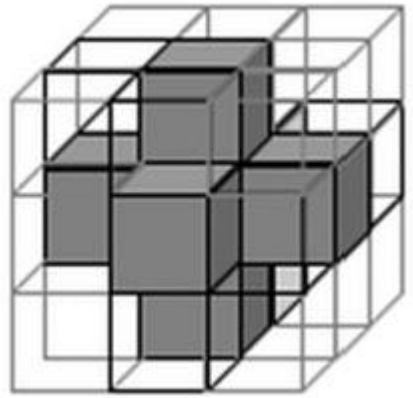

Jjumba, Anthony, and Suzana Dragicevic. "Integrating GIS-based geo-atom theory and voxel automata to simulate the dispersal of airborne pollutants." *Transactions in GIS* 19.4 (2015): 582-603.

Part 1: continuous automaton.

- Voxelate the tumour microenvironment.
- Spatial distributions of cells and matrix.
- Oxygen, nutrients, and chemotherapeutic drugs (uniform).
- Inflammation (uniform).

Part 2: discrete agents.

- Neuroblasts and Schwann cells.
- 3D von Neumann neighbourhood in the continuous automaton.

Model structure

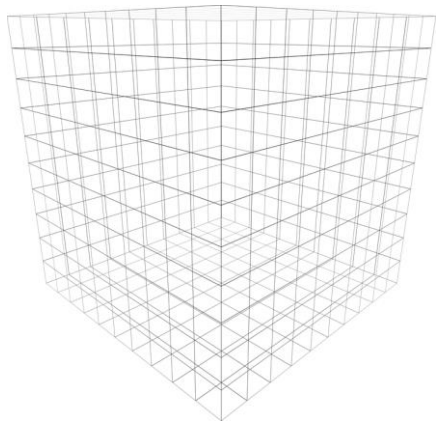

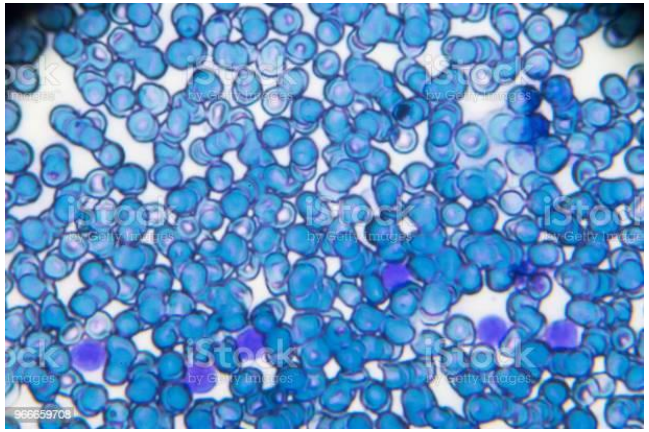

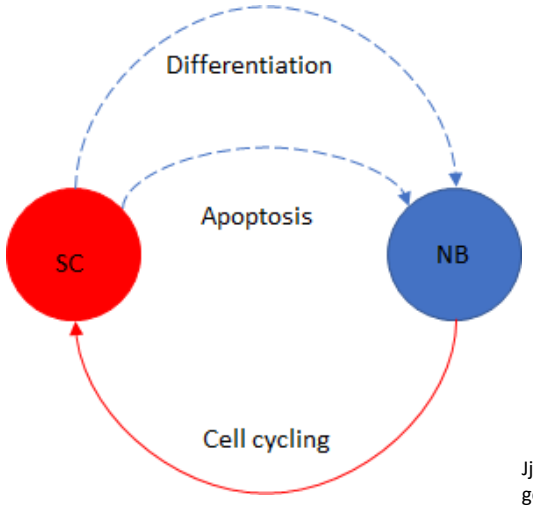

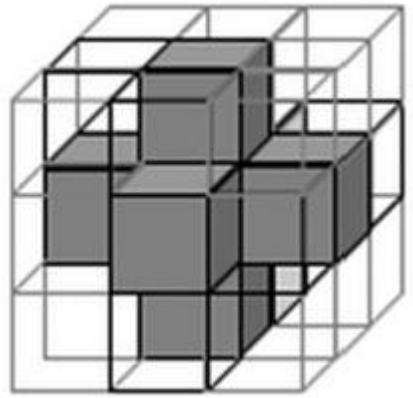

Jjumba, Anthony, and Suzana Dragicevic. "Integrating GIS-based geo-atom theory and voxel automata to simulate the dispersal of airborne pollutants." *Transactions in GIS* 19.4 (2015): 582-603.

Part 1: continuous automaton.

- Voxelate the tumour microenvironment.
- Spatial distributions of cells and matrix.
- Oxygen, nutrients, and chemotherapeutic drugs (uniform).
- Inflammation (uniform).

Part 2: discrete agents.

- Neuroblasts and Schwann cells.
- 3D von Neumann neighbourhood in the continuous automaton.
- Mutations, gene expression levels, and DNA status (short telomeres, unreplicated, and generic damage).
- Cell cycling (proliferation and division).
- Cell death (apoptosis and necrosis).

Model structure

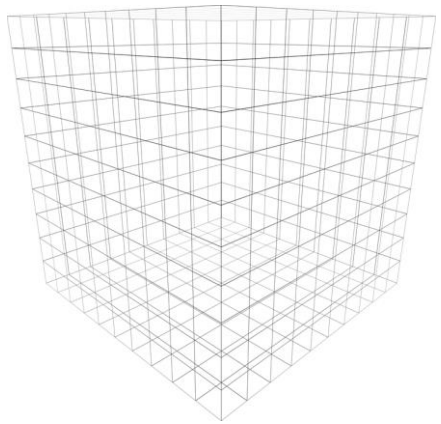

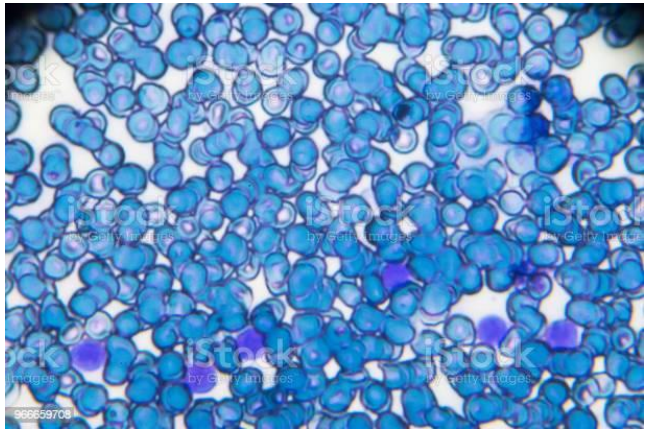

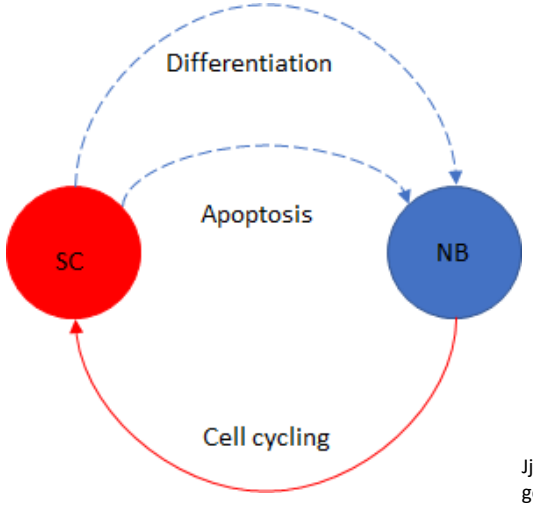

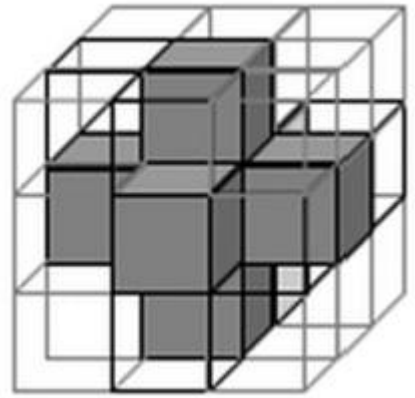

Jjumba, Anthony, and Suzana Dragicevic. "Integrating GIS-based geo-atom theory and voxel automata to simulate the dispersal of airborne pollutants." *Transactions in GIS* 19.4 (2015): 582-603.

Part 1: continuous automaton.

- Voxelate the tumour microenvironment.
- Spatial distributions of cells and matrix.
- Oxygen, nutrients, and chemotherapeutic drugs (uniform).
- Inflammation (uniform).

Part 2: discrete agents.

- Neuroblasts and Schwann cells.
- 3D von Neumann neighbourhood in the continuous automaton.
- Mutations, gene expression levels, and DNA status (short telomeres, unreplicated, and generic damage).
- Cell cycling (proliferation and division).
- Cell death (apoptosis and necrosis).

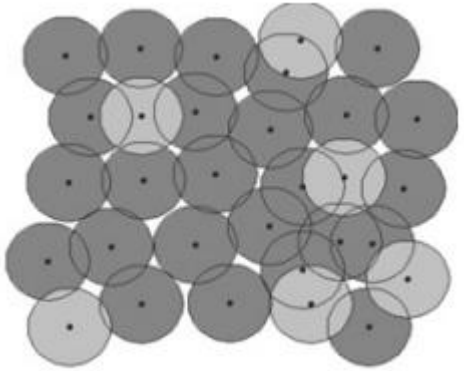

Pathmanathan, P., et al. "A computational study of discrete mechanical tissue models." *Physical biology* 6.3 (2009): 036001.

Part 3: centre-based mechanical model.

- Cell migration resolves cell-cell overlap.
- Boundary conditions and matrix abundance.

Dynamic simulation

Tumour progression is a dynamic process.

To simulate it, split the process into smaller time steps, and use the model to predict the events occurring in each time step.

1 time step = 1 hour of the patient's life.

- Evaluate each cell individually.
- Consider mechanical forces within the cell population.
- Consider how the cell population collectively affects the tumour microenvironment.

Dynamic simulation: single cell

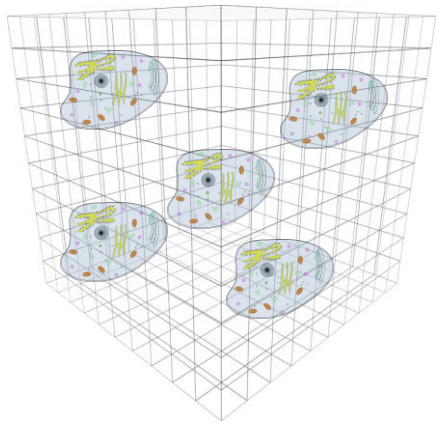

Each cell senses its microenvironment.

- Nutrients, including oxygen.
- Chemotherapeutic drugs.
- Cell counts in 3D von Neumann neighbourhood.
- Cell density (contact inhibition).

Dynamic simulation: single cell

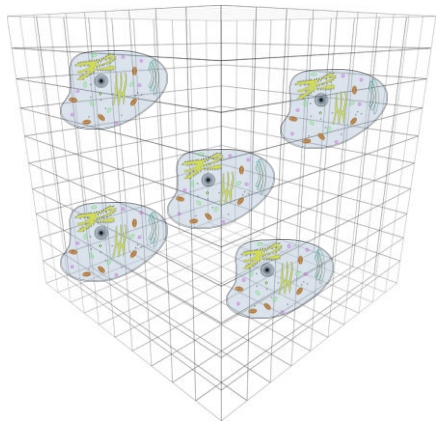

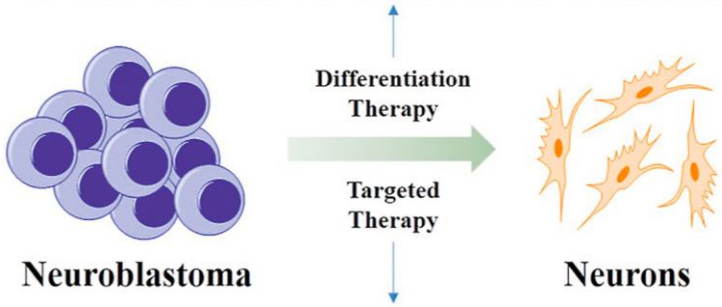

Jin, Zegao, et al. "Development of differentiation modulators and targeted agents for treating neuroblastoma." *European Journal of Medicinal Chemistry* (2020): 112818.

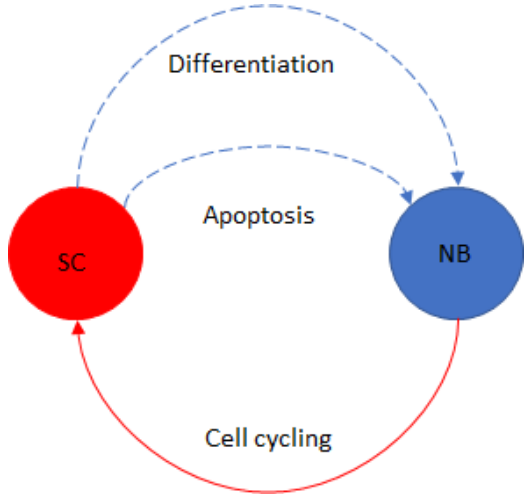

Each cell senses its microenvironment.

- Nutrients, including oxygen.
- Chemotherapeutic drugs.
- Cell counts in 3D von Neumann neighbourhood.
- Cell density (contact inhibition).

The cell modifies its behaviour.

- Differentiation.

Dynamic simulation: single cell

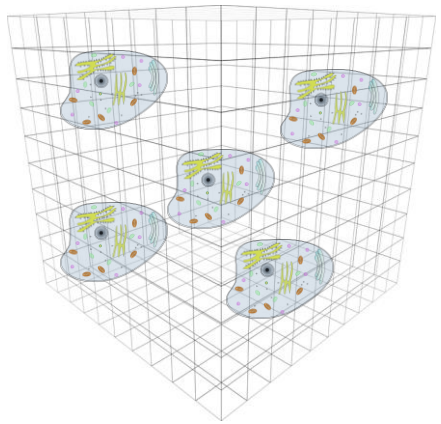

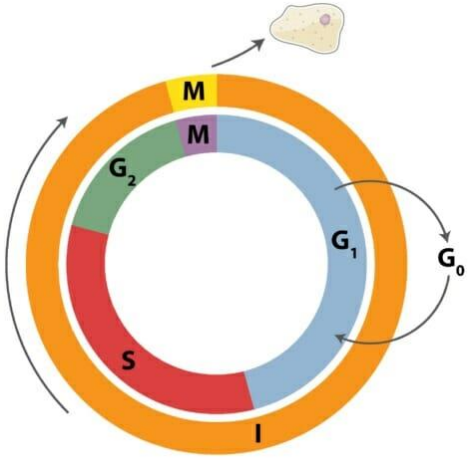

https://biologydictionary.net/cell-cycle/

Each cell senses its microenvironment.

- Nutrients, including oxygen.
- Chemotherapeutic drugs.
- Cell counts in 3D von Neumann neighbourhood.
- Cell density (contact inhibition).

The cell modifies its behaviour.

- Differentiation.
- Cycling and division.

Dynamic simulation: single cell

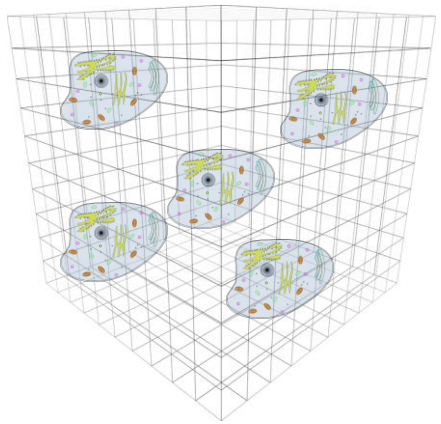

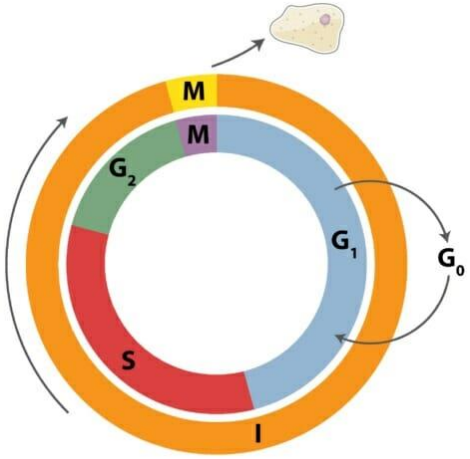

https://biologydictionary.net/cell-cycle/

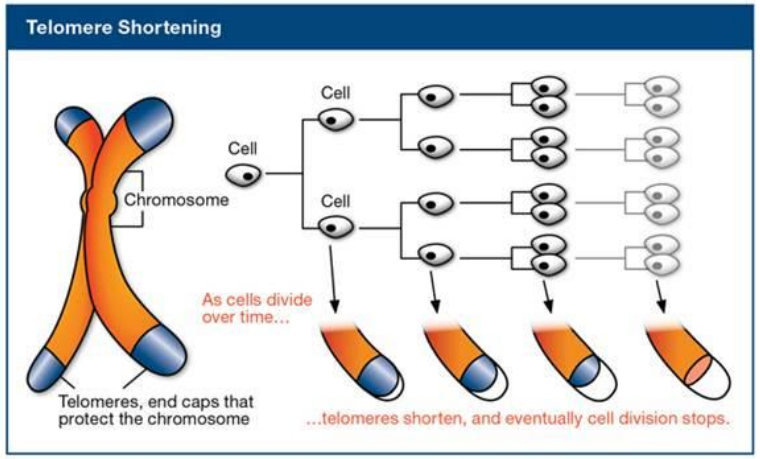

https://sphweb.bumc.bu.edu/otlt/mph-modules/ph/aging/aging3.html

Each cell senses its microenvironment.

- Nutrients, including oxygen.
- Chemotherapeutic drugs.
- Cell counts in 3D von Neumann neighbourhood.
- Cell density (contact inhibition).

The cell modifies its behaviour.

- Differentiation.
- Cycling and division.

The cell updates its attributes.

- Telomere shortening and repair.

Dynamic simulation: single cell

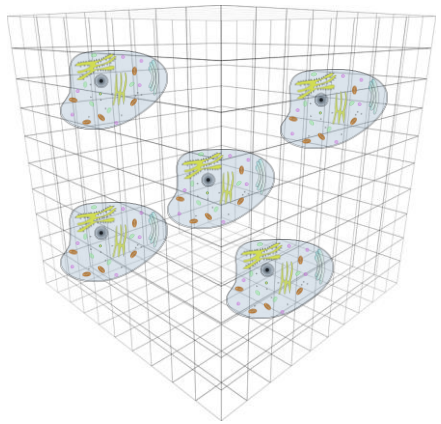

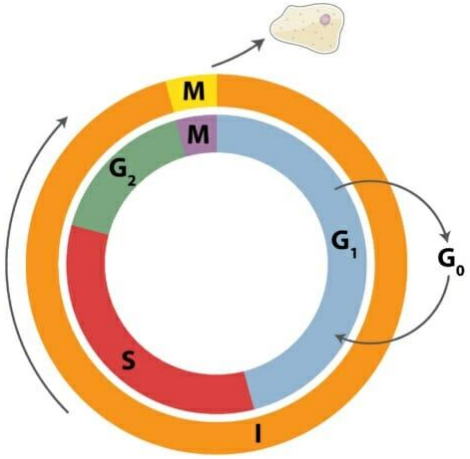

https://biologydictionary.net/cell-cycle/

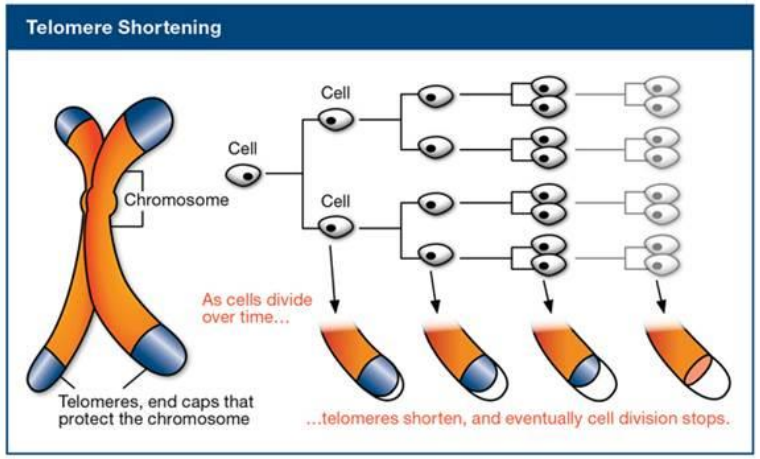

https://sphweb.bumc.bu.edu/otlt/mph-modules/ph/aging/aging3.html

Each cell senses its microenvironment.

- Nutrients, including oxygen.
- Chemotherapeutic drugs.
- Cell counts in 3D von Neumann neighbourhood.
- Cell density (contact inhibition).

The cell modifies its behaviour.

- Differentiation.
- Cycling and division.

The cell updates its attributes.

- Telomere shortening and repair.
- DNA damage and unreplicated DNA.

Dynamic simulation: single cell

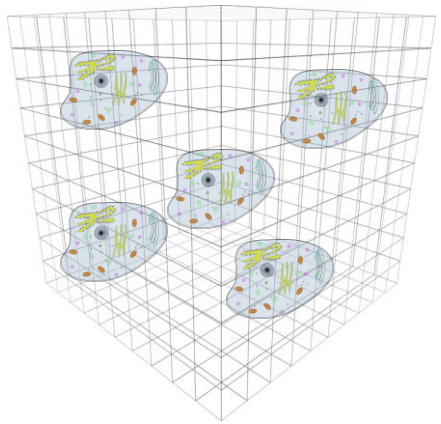

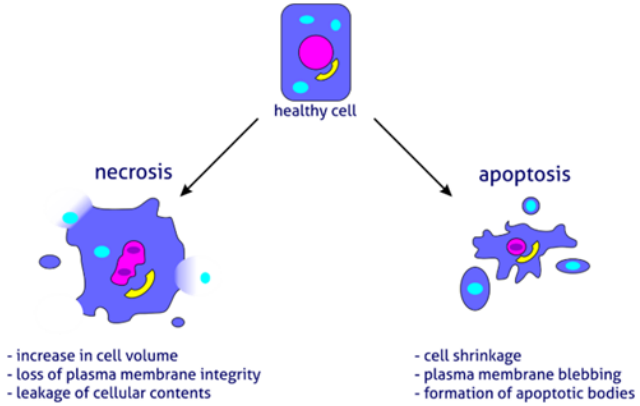

What is the difference between necrosis and apoptosis?. Ptglab.com. https://www.ptglab.com/news/blog/what-is-the-difference-between-necrosis-and-apoptosis/. Published 2021. Accessed February 24, 2021.

Each cell senses its microenvironment.

- Nutrients, including oxygen.
- Chemotherapeutic drugs.
- Cell counts in 3D von Neumann neighbourhood.
- Cell density (contact inhibition).

The cell modifies its behaviour.

- Differentiation.
- Cycling and division.
- Apoptosis and necrosis.

The cell updates its attributes.

- Telomere shortening and repair.
- DNA damage and unreplicated DNA.

Dynamic simulation: single cell

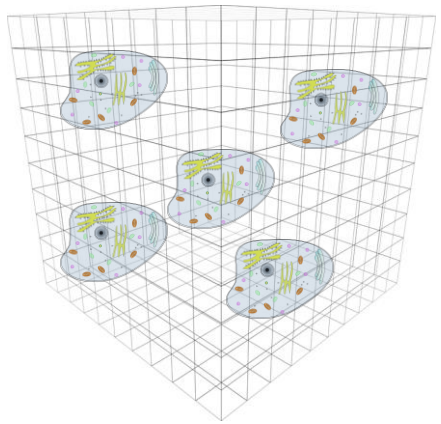

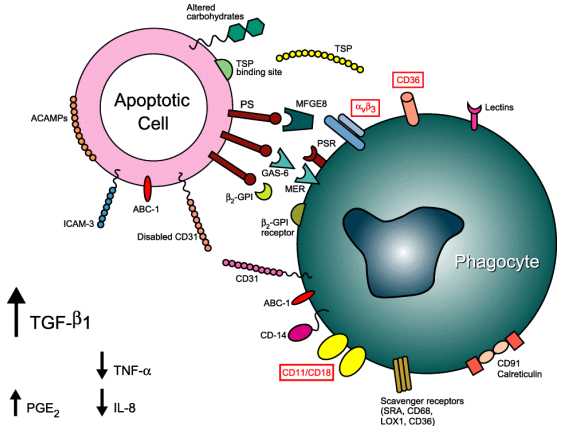

Maderna, Paola, and Catherine Godson. "Phagocytosis of apoptotic cells and the resolution of inflammation." *Biochimica et Biophysica Acta (BBA)-Molecular Basis of Disease* 1639.3 (2003): 141-151.

Each cell senses its microenvironment.

- Nutrients, including oxygen.
- Chemotherapeutic drugs.
- Cell counts in 3D von Neumann neighbourhood.
- Cell density (contact inhibition).

The cell modifies its behaviour.

- Differentiation.
- Cycling and division.
- Apoptosis and necrosis.
- Removal.

The cell updates its attributes.

- Telomere shortening and repair.
- DNA damage and unreplicated DNA.

Dynamic simulation: cell-cell repulsion

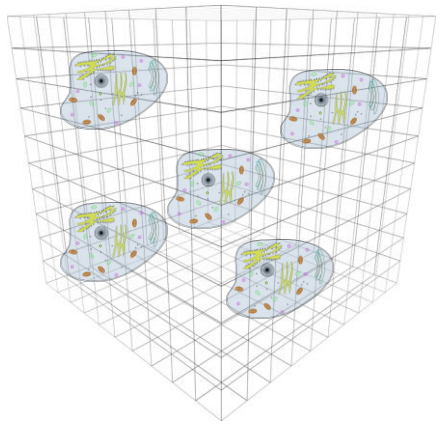

Each cell senses its microenvironment.

- Nutrients, including oxygen.
- Chemotherapeutic drugs.
- Cell counts in 3D von Neumann neighbourhood.
- **Cell density (contact inhibition).**

Dynamic simulation: cell-cell repulsion

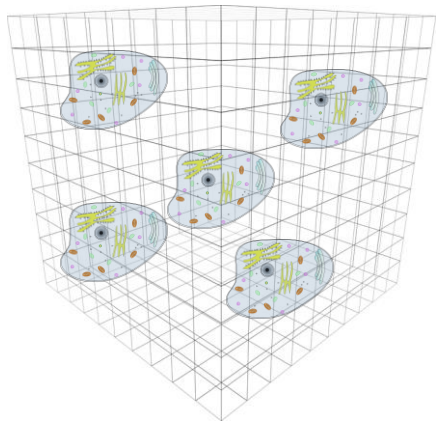

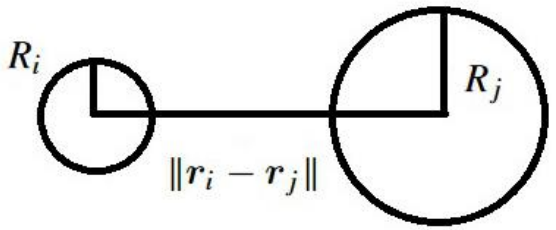

$$\delta_{ij} = R_i + R_j - \|r_i - r_j\|$$

Each cell senses its microenvironment.

- Nutrients, including oxygen.
- Chemotherapeutic drugs.
- Cell counts in 3D von Neumann neighbourhood.
- **Cell density (contact inhibition).**

Centre-Based mechanical model.

- A cell gets bigger as it progresses through the cell cycle.
- Cell-Cell overlap.

Dynamic simulation: cell-cell repulsion

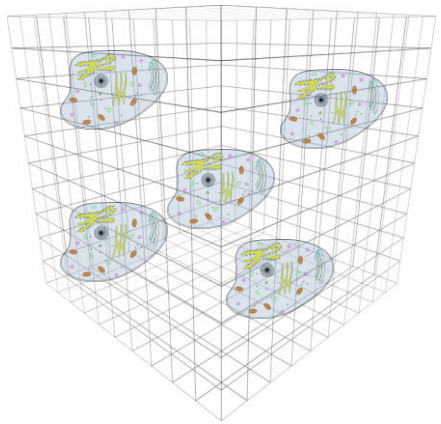

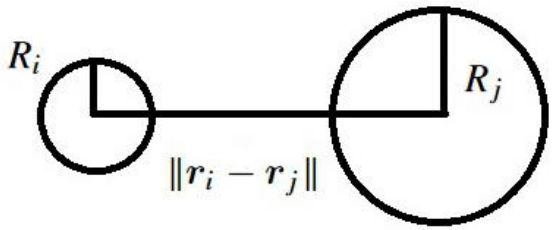

$$\delta_{ij} = R_i + R_j - \|r_i - r_j\|$$

$$\delta_i = \sum_{j=1}^{N_j} \delta_{i,j} \qquad |\boldsymbol{F_i}| = k_1 \delta_i$$

Each cell senses its microenvironment.

- Nutrients, including oxygen.
- Chemotherapeutic drugs.
- Cell counts in 3D von Neumann neighbourhood.
- **Cell density (contact inhibition).**

Centre-Based mechanical model.

- A cell gets bigger as it progresses through the cell cycle.
- Cell-Cell overlap.
- Linear force law.

Dynamic simulation: cell-cell repulsion

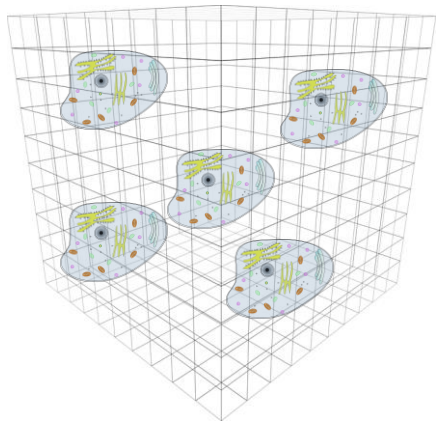

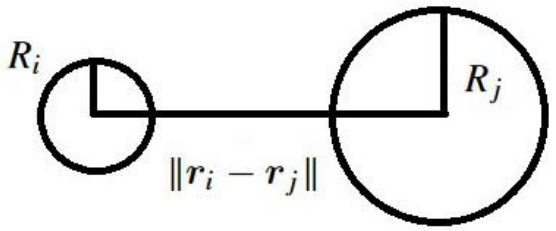

$$\delta_{ij} = R_i + R_j - \|r_i - r_j\|$$

$$\delta_i = \sum_{j=1}^{N_j} \delta_{i,j} \qquad |\boldsymbol{F_i}| = k_1 \delta_i$$

$$\boldsymbol{F_i} = \mu_{eff} \frac{d\boldsymbol{r_i}}{dt}$$

μ_{eff} scales with the abundance of matrix in the voxel.

Each cell senses its microenvironment.

- Nutrients, including oxygen.
- Chemotherapeutic drugs.
- Cell counts in 3D von Neumann neighbourhood.
- **Cell density (contact inhibition).**

Centre-Based mechanical model.

- A cell gets bigger as it progresses through the cell cycle.
- Cell-Cell overlap.
- Linear force law.
- Equation of motion.

Dynamic simulation: cell-cell repulsion

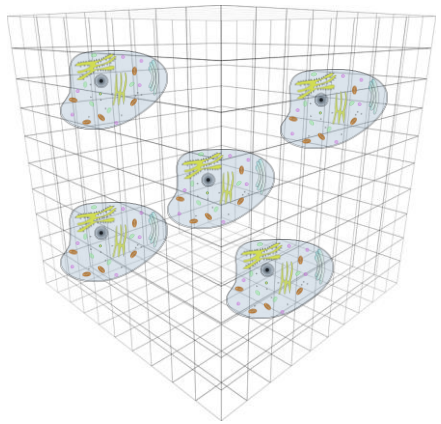

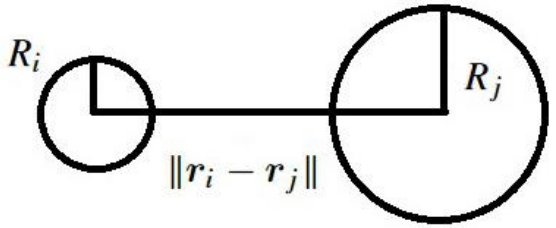

$$\delta_{ij} = R_i + R_j - \|r_i - r_j\|$$

$$\delta_i = \sum_{j=1}^{N_j} \delta_{i,j} \qquad |\boldsymbol{F_i}| = k_1 \delta_i$$

$$\boldsymbol{F_i} = \mu_{eff} \frac{d\boldsymbol{r_i}}{dt}$$

μ_{eff} scales with the abundance of matrix in the voxel.

Each cell senses its microenvironment.

- Nutrients, including oxygen.
- Chemotherapeutic drugs.
- Cell counts in 3D von Neumann neighbourhood.
- **Cell density (contact inhibition).**

Centre-Based mechanical model.

- A cell gets bigger as it progresses through the cell cycle.
- Cell-Cell overlap.
- Linear force law.
- Equation of motion.

Iterate these steps until convergence.

Dynamic simulation: collective phenomena

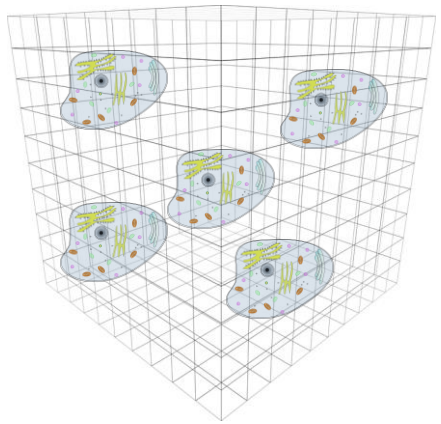

Each cell senses its microenvironment.

- Nutrients, including oxygen.
- Chemotherapeutic drugs.
- Cell counts in 3D von Neumann neighbourhood.
- Cell density (contact inhibition).

The cells modify their microenvironment.

- Consume nutrients.
- Remodel the vasculature.
- Produce matrix.

Procedures in one time step

1. Each cell senses its microenvironment, modifies its behaviour, and updates its attributes.

2. Resolve cell-cell overlap using the centre-based mechanical model.

3. The cells collectively modify their microenvironment.

Objectives

1. PRIMAGE project.

2. Scale separation strategy in the project.

3. The first multi-cellular model of neuroblastoma.

4. Model calibration using GPUs.

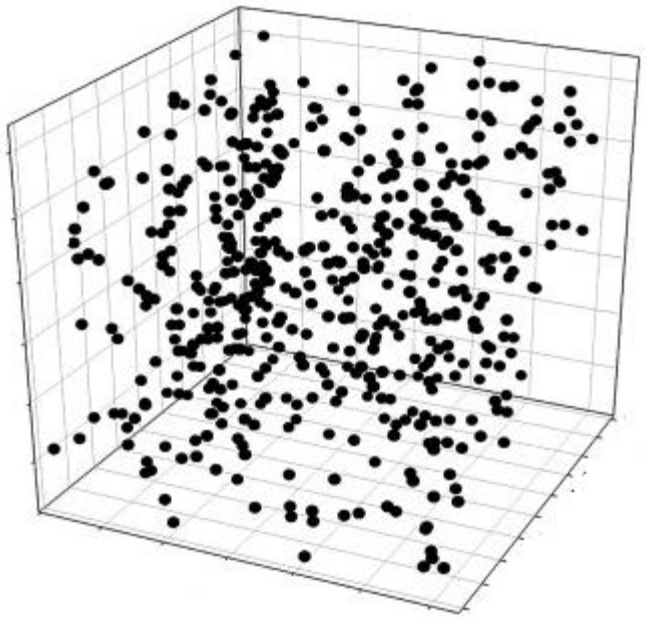

Lack of relevant data.

- 20 fitting parameters.
- 3000 parametric combinations generated by Latin hypercube sampling.

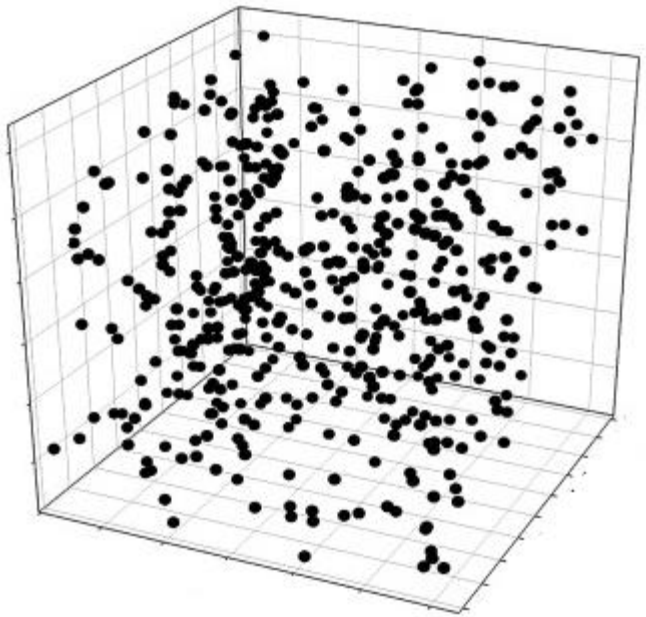

Lack of relevant data.

- 20 fitting parameters.
- 3000 parametric combinations generated by Latin hypercube sampling.

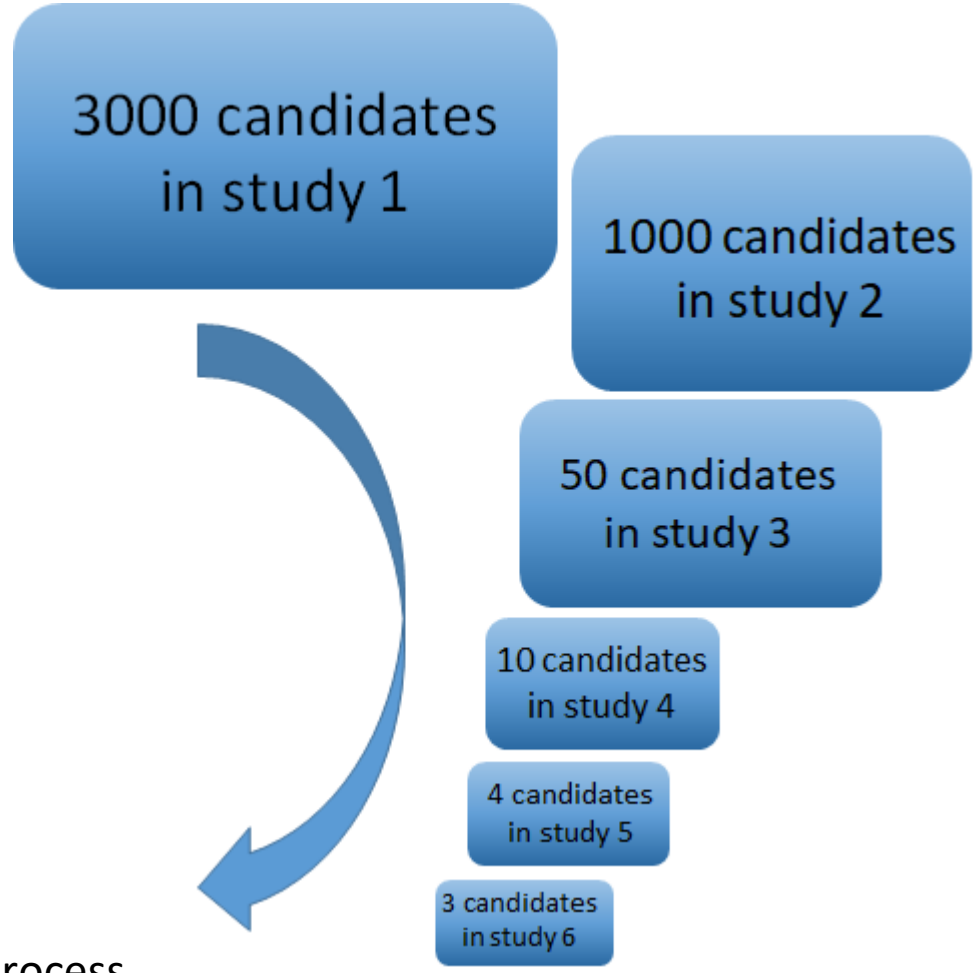

Selection process.

- Eliminated the 3000 candidates gradually in a tournament of 6 studies.
- Experiments and clinical observations.
- The set of parameters that describe the experiments and observations best.

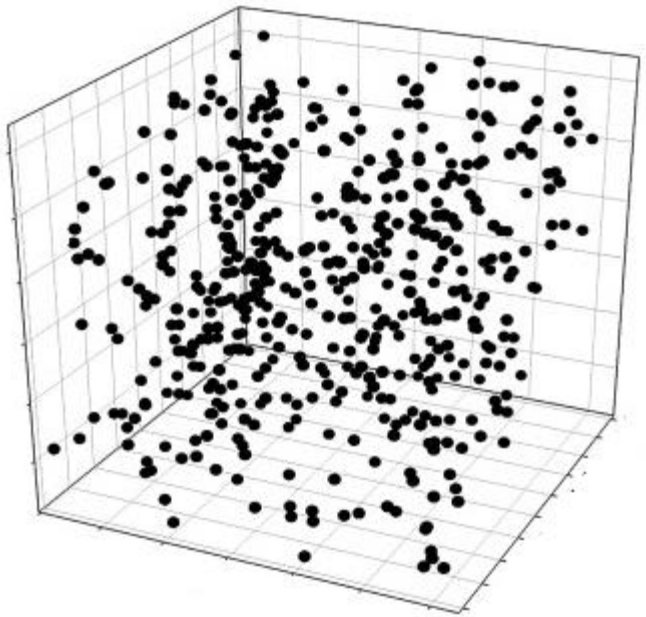

Squid Game. Created by Hwang Dong-hyuk, Netflix, 2021.

Lack of relevant data.

- 20 fitting parameters.
- 3000 parametric combinations generated by Latin hypercube sampling.

Selection process.

- 6 studies mimicking experiments and clinical observations.
- The parameters that describe the experiments and observations best.

[CANCER RESEARCH 30, 2110–2118, August 1970]

Definition of a Continuous Human Cell Line Derived from Neuroblastoma[1]

Joseph J. Tumilowicz, Warren W. Nichols, Jolanta J. Cholon, and Arthur E. Greene

Departments of Cytogenetics [J. J. T., W. W. N., J. J. C.], and Cell Biology [A. E. G.], Institute for Medical Research, Camden, New Jersey 08103

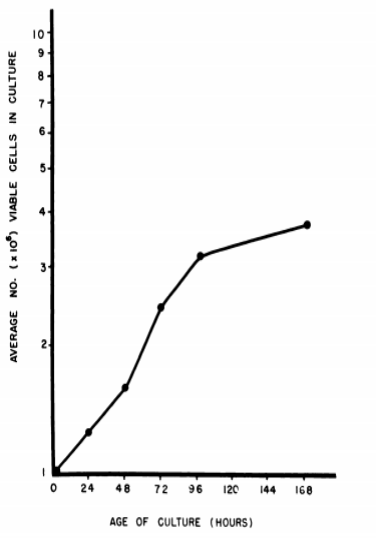

Squid Game. Created by Hwang Dong-hyuk, Netflix, 2021.

Study 1.

- Cell line derived from neuroblastoma tissue was grown in a growth medium.
- The cell population was tracked over time using hemocytometer.

Results.

- Used each parametric combination to simulate tumour growth.
- Data fitting: residual sum of squares.
- Eliminated bottom 2000 combinations.

$$\mathrm{RSS} = \sum_{i=1}^{n} (y_i - f(x_i))^2$$

Physics in Medicine & Biology

PAPER • OPEN ACCESS

The role of necrosis, acute hypoxia and chronic hypoxia in ^{18}F-FMISO PET image contrast: a computational modelling study

Daniel R Warren[1] and Mike Partridge[1]

Published 23 November 2016 • © 2016 Institute of Physics and Engineering in Medicine

Physics in Medicine & Biology, Volume 61, Number 24

Citation Daniel R Warren and Mike Partridge 2016 *Phys. Med. Biol.* **61** 8596

	Three-stage fit	95% CI	Direct fit	95% CI
Maximum oxygen consumption rate, q_{max} (mmHg · s^{-1})	17.5	15.3–25.1	16.3	15.3–17.9
P_{O_2} for 50% drop in consumption, $P_{50,q}$ (mmHg)	2.7	0.0–12.5	1.6	1.2–2.1
Maximum misonidazole binding rate, $k_{b,0}$ ($\times 10^{-4}$ s^{-1})	4.5	3.9–4.9	4.4	2.5–5.3
P_{O_2} for 50% drop in binding, $P_{50,b}$ (mmHg)	1.4	0.3–2.6	1.4	1.1–2.5
P_{O_2} for 50% necrosis, $P_{50,n}$ (mmHg)	1.2	0.1–4.9	1.0	0.4–1.2

Squid Game. Created by Hwang Dong-hyuk, Netflix, 2021.

Study 2.

- Data-driven modelling study.
- Oxygen level at which 50 % of cells will die due to hypoxia.

Results.

- Used each parametric combination to simulate hypoxia.
- Death rate: how close to 50 %.
- Combined the results of studies 1 and 2.
- Top 50 combinations remained.

Medical and Pediatric Oncology 36:163–168 (2001)

Neuroblastoma Cells Provoke Schwann Cell Proliferation In Vitro

Ingeborg M. Ambros, MD,[1]* Andishe Attarbaschi, MD,[1] Silvia Rumpler,[1]
Andrea Luegmayr,[1] Edvin Turkof, MD,[2] Helmut Gadner, MD,[1] and
Peter F. Ambros, PhD[1]

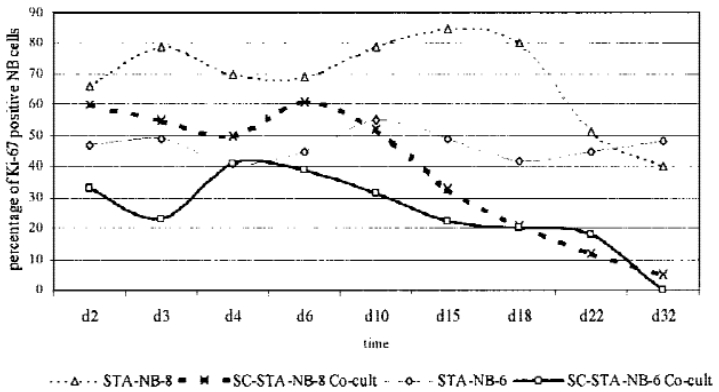

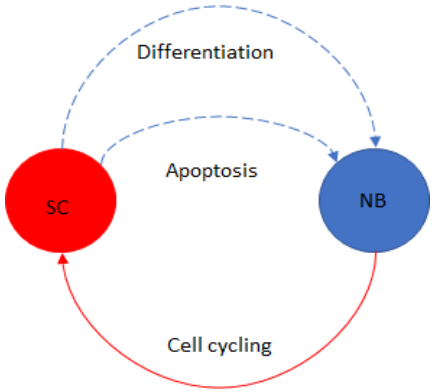

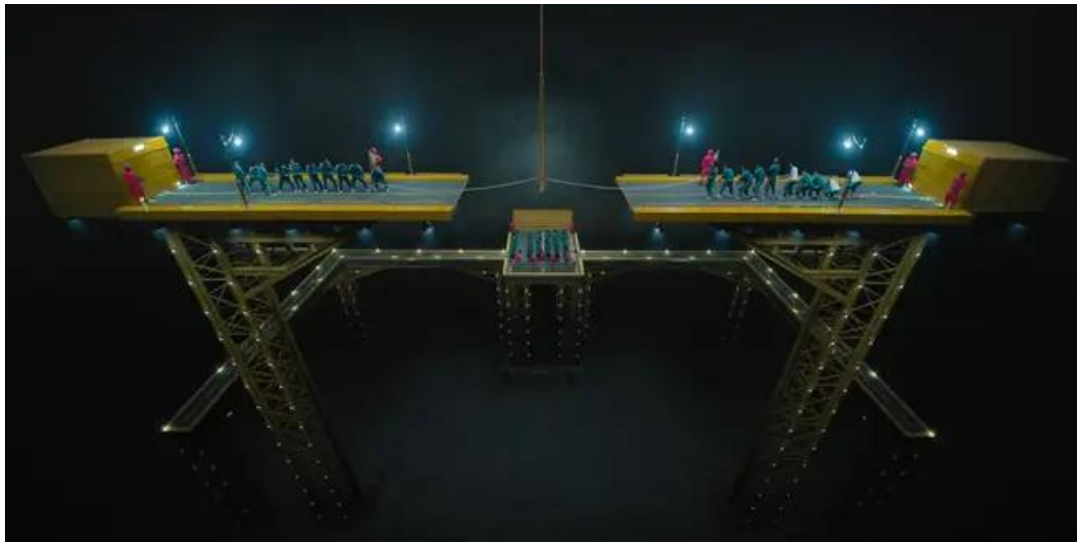

Squid Game. Created by Hwang Dong-hyuk, Netflix, 2021.

Study 3.

- Neuroblasts and Schwann cells were cocultivated.
- Fractions of proliferating neuroblasts and Schwann cells were tracked over time.
- Fraction of apoptotic neuroblasts was also measured at a point in time.

Results.

- Used each parametric combination to simulate the dynamics between the neuroblasts and Schwann cells.
- Data fitting: 3 residual sums of squares.
- Top 10 combinations remained.

$$\mathrm{RSS} = \sum_{i=1}^{n} (y_i - f(x_i))^2$$

Pediatr Blood Cancer 2009;53:563–569

Clinicopathological Characteristics of Ganglioneuroma and Ganglioneuroblastoma: A Report From the CCG and COG

Chizuko Okamatsu, MD,[1,2] Wendy B. London, PhD,[3] Arlene Naranjo, PhD,[3] Michael D. Hogarty, MD,[4] Julie M. Gastier-Foster, PhD,[5,6] A. Thomas Look, MD,[7] Michael LaQuaglia, MD,[8] John M. Maris, MD,[4] Susan L. Cohn, MD,[9] Katherine K. Matthay, MD,[10] Robert C. Seeger, MD,[11] Tsutomu Saji, MD,[2] and Hiroyuki Shimada, MD, PhD[1]*

TABLE V. Event-Free and Overall Survival for Tumor Category by Clinical Stage

Histological category	Overall, number of patients	Number with survival data	5-year, EFS ± SE (%)	EFS, *P*-value	5-year, OS ± SE (%)	OS, *P*-value
GN-maturing						
Stage 1, 2, 3	36	34	100		100	
Stage 4	0	0	—	NA	—	NA
GNB-intermixed						
Stage 1, 2, 3	187	179	94.1 ± 4.3		97.0 ± 3.2	
Stage 4	2	2	—	NA	—	NA
GNB-nodular FS						
Stage 1, 2, 3	56	55	92.6 ± 6.3		100	
Stage 4	3	3	100	NA	100	NA
GNB-nodular US						
Stage 1, 2, 3	116	114	80.1 ± 8.0		86.2 ± 7.0	
Stage 4	132	132	16.7 ± 5.8	<0.0001	35.9 ± 7.0	<0.0001

EFS, event-free survival; OS, overall survival; SE, standard error; NA, not applicable due to no event; —, No patients at risk at 5 years; GN-maturing, ganglioneuroma, maturing subtype; GNB-intermixed, ganglioneuroblastoma, intermixed; GNB-nodular FS, ganglioneuroblastoma, nodular—favorable subset; GNB-nodular US, ganglioneuroblastoma, nodular—unfavorable subset.

Squid Game. Created by Hwang Dong-hyuk, Netflix, 2021.

Study 4.

- Clinical observations.
- Neuroblastoma, nodular ganglioneuroblastoma, intermixed ganglioneuroblastoma, maturing ganglioneuroma, and mature ganglioneuroma.
- Clinical outcomes: regression, differentiation, and malignant (death, progression, and relapse).

Results.

- Used each parametric combination to predict the clinical outcomes for different histology types.
- Proportion of malignant outcomes.
- Only 4 combinations gave results resembling clinical observations.

A mechanistic classification of clinical phenotypes in neuroblastoma

Sandra Ackermann[1,2*], Maria Cartolano[2,3*], Barbara Hero[4], Anne Welte[1,2], Yvonne Kahlert[1,2], Andrea Roderwieser[1,2], Christoph Bartenhagen[1,2], Esther Walter[1,2], Judith Gecht[4], Laura Kerschke[5], Ruth Volland[4], Roopika Menon[6], Johannes M. Heuckmann[6], Moritz Gartlgruber[7], Sabine Hartlieb[7], Kai-Oliver Henrich[7], Konstantin Okonechnikov[8], Janine Altmüller[2,9], Peter Nürnberg[2,9,10], Steve Lefever[11], Bram de Wilde[11], Frederik Sand[1,2], Fakhera Ikram[1,2,12], Carolina Rosswog[1,2], Janina Fischer[1,2], Jessica Theissen[1,4], Falk Hertwig[1,2,13,14,15], Aatur D. Singhi[16], Thorsten Simon[4], Wenzel Vogel[17,18], Sven Perner[17,18], Barbara Krug[19], Matthias Schmidt[20], Sven Rahmann[21,22], Viktor Achter[23], Ulrich Lang[23,24], Christian Vokuhl[25], Monika Ortmann[26], Reinhard Büttner[26], Angelika Eggert[13,14,15], Frank Speleman[11], Roderick J. O'Sullivan[27], Roman K. Thomas[3,14,26,28], Frank Berthold[4*], Jo Vandesompele[11*], Alexander Schramm[29*], Frank Westermann[7*], Johannes H. Schulte[13,14,15,28*], Martin Peifer[2,3*], Matthias Fischer[1,2*†]

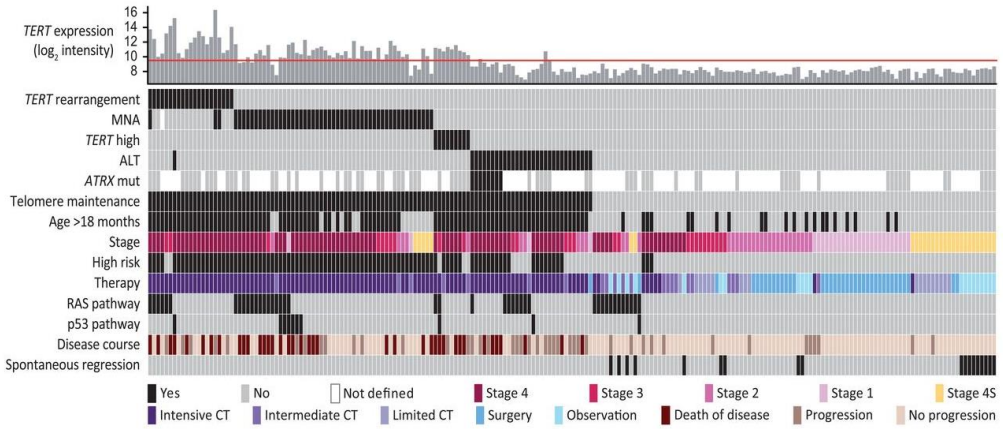

Squid Game. Created by Hwang Dong-hyuk, Netflix, 2021.

Study 5.

- Clinical observations.
- Different combinations of mutations.
- MYCN not amplified.
- Clinical outcomes: regression, differentiation, and malignant (death, progression, and relapse).

Results.

- Used each parametric combination to predict the clinical outcomes given different mutations.
- Proportion of malignant outcomes.
- Only 3 combinations gave results resembling clinical observations.

A mechanistic classification of clinical phenotypes in neuroblastoma

Sandra Ackermann[1,2*], Maria Cartolano[2,3*], Barbara Hero[4], Anne Welte[1,2], Yvonne Kahlert[1,2], Andrea Roderwieser[1,2], Christoph Bartenhagen[1,2], Esther Walter[1,2], Judith Gecht[4], Laura Kerschke[5], Ruth Volland[4], Roopika Menon[6], Johannes M. Heuckmann[6], Moritz Gartlgruber[7], Sabine Hartlieb[7], Kai-Oliver Henrich[7], Konstantin Okonechnikov[8], Janine Altmüller[2,9], Peter Nürnberg[2,9,10], Steve Lefever[11], Bram de Wilde[11], Frederik Sand[1,2], Fakhera Ikram[1,2,12], Carolina Rosswog[1,2], Janina Fischer[1,2], Jessica Theissen[1,4], Falk Hertwig[1,2,13,14,15], Aatur D. Singhi[16], Thorsten Simon[4], Wenzel Vogel[17,18], Sven Perner[17,18], Barbara Krug[19], Matthias Schmidt[20], Sven Rahmann[21,22], Viktor Achter[23], Ulrich Lang[23,24], Christian Vokuhl[25], Monika Ortmann[26], Reinhard Büttner[26], Angelika Eggert[13,14,15], Frank Speleman[11], Roderick J. O'Sullivan[27], Roman K. Thomas[3,14,26,28], Frank Berthold[4*], Jo Vandesompele[11*], Alexander Schramm[29*], Frank Westermann[7*], Johannes H. Schulte[13,14,15,28*], Martin Peifer[2,3*], Matthias Fischer[1,2*†]

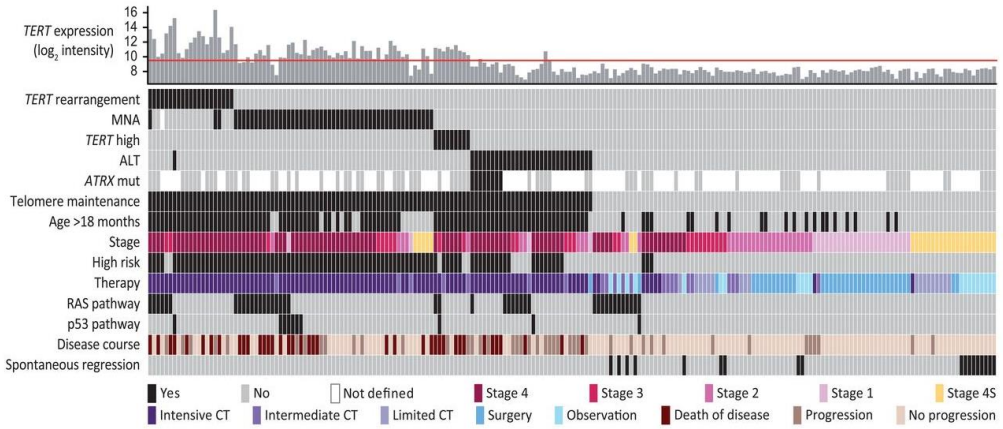

Study 6.

- Clinical observations.
- Different combinations of mutations.
- **MYCN amplified.**
- Clinical outcomes: regression, differentiation, and malignant (death, progression, and relapse).

Squid Game. Created by Hwang Dong-hyuk, Netflix, 2021.

Results.

- Used each parametric combination to predict the clinical outcomes given different mutations.
- Proportion of malignant outcomes.
- **Results not conclusive.**
- **All studies taken together, candidate 564 was selected.**

A mechanistic classification of clinical phenotypes in neuroblastoma

Sandra Ackermann[1,2*], Maria Cartolano[2,3*], Barbara Hero[4], Anne Welte[1,2], Yvonne Kahlert[1,2], Andrea Roderwieser[1,2], Christoph Bartenhagen[1,2], Esther Walter[1,2], Judith Gecht[4], Laura Kerschke[5], Ruth Volland[4], Roopika Menon[6], Johannes M. Heuckmann[6], Moritz Gartlgruber[7], Sabine Hartlieb[7], Kai-Oliver Henrich[7], Konstantin Okonechnikov[8], Janine Altmüller[2,9], Peter Nürnberg[2,9,10], Steve Lefever[11], Bram de Wilde[11], Frederik Sand[1,2], Fakhera Ikram[1,2,12], Carolina Rosswog[1,2], Janina Fischer[1,2], Jessica Theissen[1,4], Falk Hertwig[1,2,13,14,15], Aatur D. Singhi[16], Thorsten Simon[4], Wenzel Vogel[17,18], Sven Perner[17,18], Barbara Krug[19], Matthias Schmidt[20], Sven Rahmann[21,22], Viktor Achter[23], Ulrich Lang[23,24], Christian Vokuhl[25], Monika Ortmann[26], Reinhard Büttner[26], Angelika Eggert[13,14,15], Frank Speleman[11], Roderick J. O'Sullivan[27], Roman K. Thomas[3,14,26,28], Frank Berthold[4*], Jo Vandesompele[11*], Alexander Schramm[29*], Frank Westermann[7*], Johannes H. Schulte[13,14,15,28*], Martin Peifer[2,3*], Matthias Fischer[1,2*†]

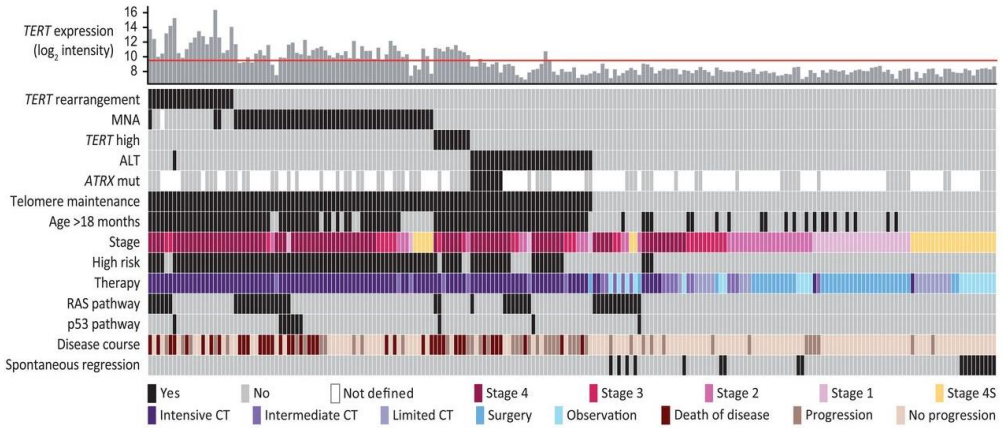

Index	MYCN_fn	MAPK_RA	MAPK_RA	p53_fn	p73_fn	HIF_fn	P_cycle_s	P_DNA_da	P_DNA_c
677	0.277863	0.296396	0.081294	0.121137	0.168345	0.943243	0.529251	0.222474	0.990451
184	0.484521	0.518488	0.252074	0.676754	0.436464	0.658059	0.519606	0.614104	0.766484
2991	0.301635	0.87196	0.421385	0.797464	0.786514	0.234779	0.385223	0.219635	0.925318
825	0.892225	0.787593	0.215333	0.856983	0.718434	0.925868	0.25681	0.292857	0.988103
564	0.942648	0.377628	0.003161	0.19809	0.141042	0.59177	0.344412	0.772948	0.77149
1540	0.245592	0.997054	0.615927	0.603909	0.193378	0.311584	0.328683	0.659884	0.814463
2193	0.761934	0.675797	0.390508	0.893939	0.19777	0.760859	0.975454	0.337441	0.96006
1556	0.501221	0.879769	0.545846	0.085968	0.131161	0.13793	0.158815	0.126268	0.498999
675	0.69287	0.529858	0.232187	0.806742	0.69036	0.254842	0.541578	0.989668	0.971362
1892	0.547878	0.673346	0.579237	0.132174	0.816287	0.973364	0.553501	0.631952	0.871724
2307	0.832634	0.59399	0.204702	0.913315	0.654981	0.393086	0.472165	0.259098	0.902943
2198	0.485041	0.909258	0.218517	0.203592	0.042106	0.460479	0.623141	0.795116	0.958733
1106	0.815031	0.984735	0.400839	0.28017	0.267183	0.39705	0.947455	0.01568	0.105446

Study 6.

- Clinical observations.
- Different combinations of mutations.
- **MYCN amplified.**
- Clinical outcomes: regression, differentiation, and malignant (death, progression, and relapse).

Results.

- Used each parametric combination to predict the clinical outcomes given different mutations.
- Proportion of malignant outcomes.
- **Results not conclusive.**
- **All studies taken together, candidate 564 was selected.**

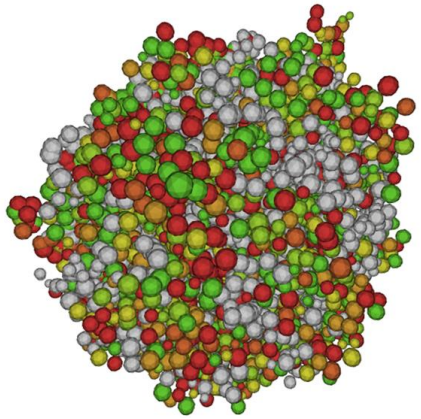

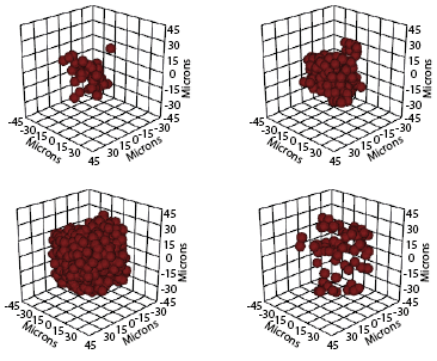

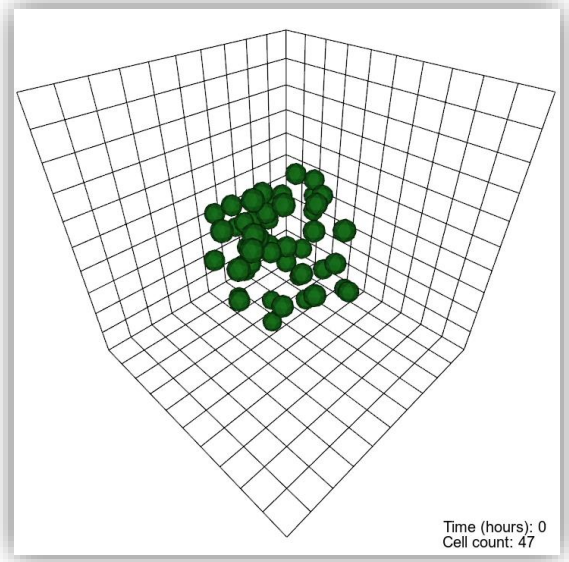

FLAME GPU

High computational costs.

- Millions of cells in > 4 months.
- Stochastic simulations.

High-Performance computing.

- Simulations on GPUs enabled by FLAMEGPU.
- Mapping of model descriptions to optimised CUDA code.

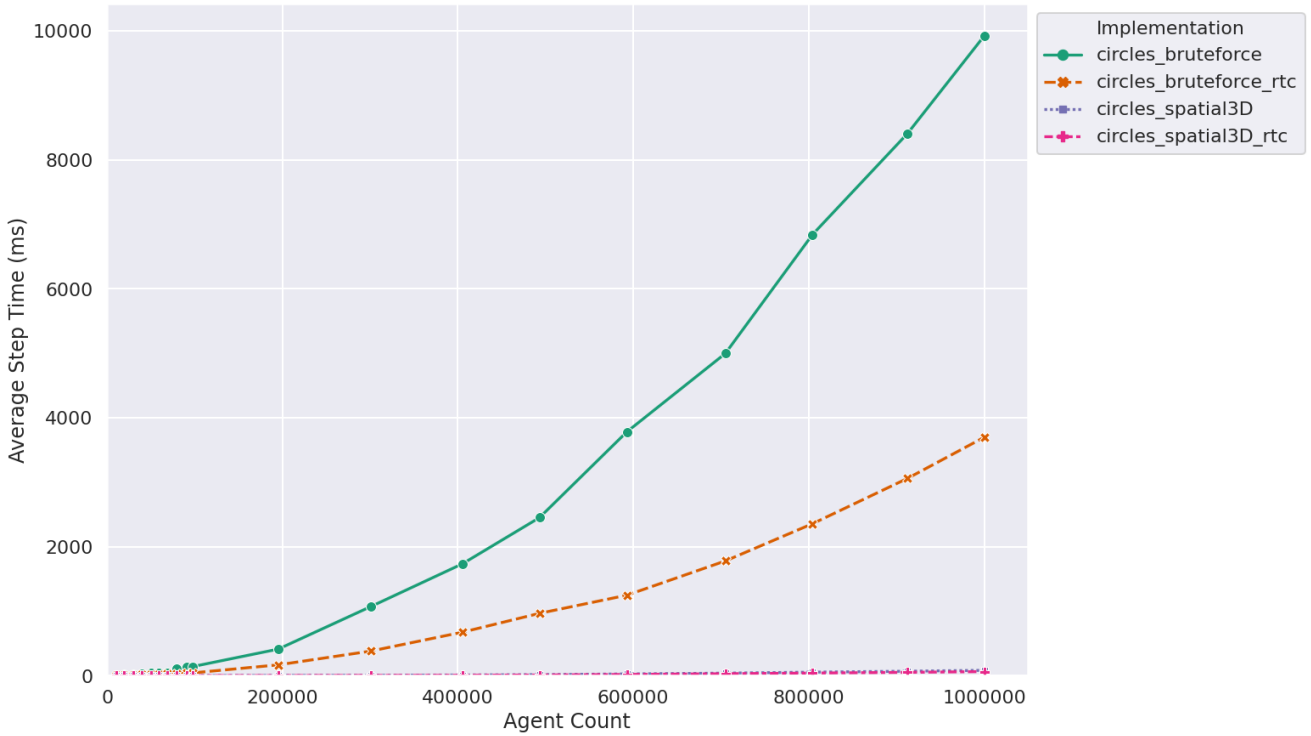

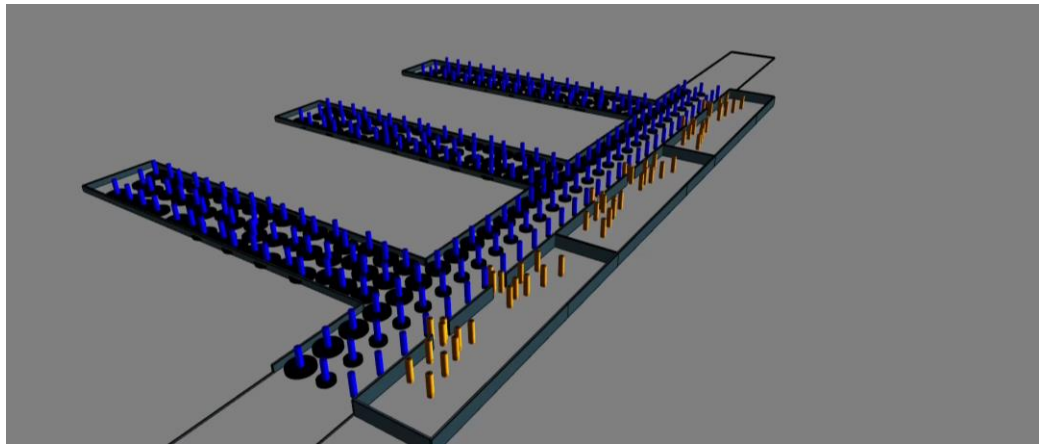

FLAMEGPU2.

- Modellers can focus on building the model without worrying about CUDA programming and GPU optimisation strategies.
- High performance: millions of agents.
- Visualisation in real time.
- C++ and Python APIs for model definition.

Applications.

- Neuroblastoma progression.
- Development of *in silico* trials for tuberculosis (Strituvad). 13 agent types, around 170 functions, and over 200 parameters.
- Understanding boarding and alighting at platform-train interface under social distancing guidelines.

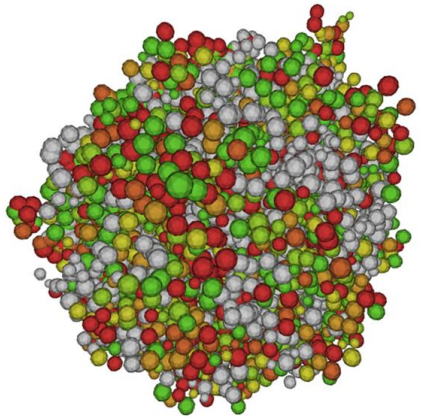

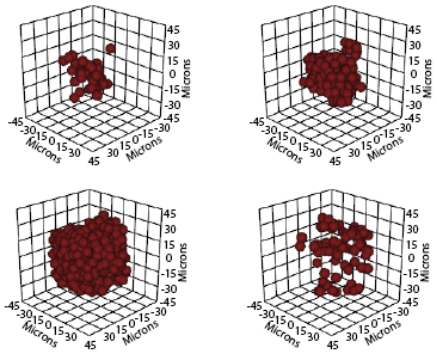

Computational time.

- 2 TITAN V GPUs, 1 TITAN XP GPU, and 1 TITAN RTX GPU.
- 3000 time steps took 5 to 10 minutes.
- **All 6 studies took around 40 days.**
- Impossible without GPUs.

FLAME GPU

High computational costs.

- Millions of cells in > 4 months.
- Stochastic simulations.

High-Performance computing.

- Simulations on GPUs enabled by FLAMEGPU.
- Mapping of model descriptions to optimised CUDA code.

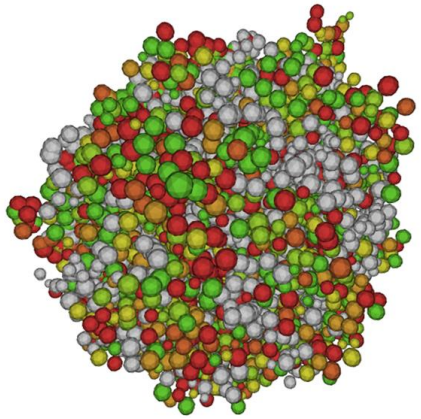

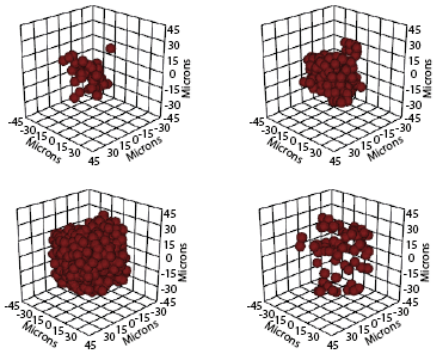

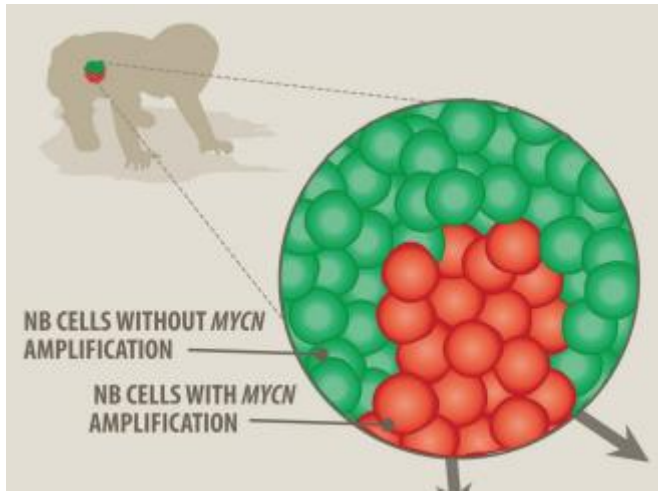

Bogen, Dominik, et al. "The genetic tumor background is an important determinant for heterogeneous MYCN-amplified neuroblastoma." *International journal of cancer* 139.1 (2016): 153-163.

FLAME GPU

High computational costs.

- Millions of cells in > 4 months.
- Stochastic simulations.

High-Performance computing.

- Simulations on GPUs enabled by FLAMEGPU.
- Mapping of model descriptions to optimised CUDA code.

Next steps.

- Introduce clones of cells with different mutations and simulate tumour progression.
- What are the factors that contribute to regression/differentiation?
- How can we manipulate these factors to induce regression/differentiation?

Take-Home Message 1.

The PRIMAGE project aims to build a decision support system for the clinical management of malignant solid tumours.

Take-Home Message 2.

Cancer hallmarks span 9 orders of magnitude in both space and time. Due to limits posed by experimental resolutions, model complexity, and computational costs, it is necessary to build separate models for the critical scales and orchestrate information flow between the models.

Take-Home Message 3.

We built the very first multi-cellular model of neuroblastoma by integrating a continuous automaton, discrete agents, and a centre-based mechanical model.

Take-Home Message 4.

The multi-cellular model has 20 fitting parameters. We calibrated them in a Squid Game–style tournament. We used Latin hypercube sampling to generate 3000 combinations of parameters, aggregated experimental and clinical data, and used the data to design 6 *in silico* studies performed on GPUs to assess the combinations.

RUDN university

UNIVERSITÉ DE LYON

International online workshop

Mathematical Modelling in Biomedicine

October 25 – 29, 2021 Moscow, Russia

The University Of Sheffield.

INSIGNEO

Institute for *in silico* Medicine

PRIMAGE

Medical imaging
Artificial intelligence
Childhood cancer research

Horizon 2020
European Union Funding
for Research & Innovation